J. Fluid Mech. (1979), *vol.* 94, *part* 4, *pp.* 729–744
Printed in Great Britain

The interaction of sound with low Mach number wall turbulence, with application to sound propagation in turbulent pipe flow

By M. S. HOWE

Bolt Beranek and Newman, Inc., 50 Moulton Street, Cambridge, Massachusetts 02138

(Received 21 December 1978)

This paper discusses the influence of turbulence convection on the formation of acoustic momentum and thermal boundary layers over a rigid surface in the presence of a low Mach number wall-turbulence shear flow. Equations which determine the modified boundary-layer profiles are obtained from a consideration of the relaxation of coherent perturbations in the Reynolds stress. These equations can be solved analytically for a wide range of conditions which are investigated in detail. The theory is applied to the problem of sound propagation in fully-developed turbulent pipe flow, and at low Mach numbers good agreement is obtained between predicted acoustic attenuation rates and experimental results available in the literature.

1. Introduction

There are two principal mechanisms by which sound is attenuated by turbulence. The first is radiation damping, whereby secondary sound waves are produced and scattered out of the line of propagation of the incident sound (Lighthill 1953; Kraichnan 1953; Batchelor 1957; Howe 1973). This tends to dominate at frequencies exceeding that characteristic of the turbulent fluctuations. At lower frequencies, corresponding to acoustic wavelengths greatly in excess of the turbulence correlation scale, the attenuation is caused by a direct transfer of energy to the turbulence (Noir & George 1978). In this case the periodic straining of turbulent vortex lines by the sound cannot be regarded as reversible, there being sufficient time in an acoustic cycle for energy to be re-distributed amongst the various degrees of freedom of the turbulence through their nonlinear couplings.

The thermo-viscous attenuation of sound (caused by molecular diffusion) is known to increase significantly in the presence of rigid surfaces, such as when sound propagates within a tube. It might be anticipated, therefore, that low frequency attenuation associated with turbulence relaxation would be similarly enhanced. This is confirmed by the experiments of Ahrens & Ronneberger (1971) and of Ingard & Singhal (1974) involving standing waves in turbulent pipe flows. Velocity gradients are large near the pipe wall, and the dominant turbulence relaxation processes would accordingly be expected to occur within the turbulent wall layers, and to be equivalent to an acoustic modulation of the shear stress exerted on the pipe. Ingard & Singhal assumed that the modulation frequency was so low that the properties of the mean turbulent flow over the whole cross-section of the pipe could be taken to vary in a quasi-static manner, corresponding to a slow fluctuation in the mean velocity. This hypothesis leads to a

0022-1120/79/4302-7500 $02.00

semi-empirical formula for the attenuation which involves the mean velocity in the pipe, but exhibits no dependence on the acoustic frequency. In this respect their approach is analogous to that underlying Bradshaw's (1967) analysis of turbulent boundary-layer surface stress fluctuations produced by large-scale 'inactive' components of the turbulent field.

In this paper the question of the interaction of sound with a turbulent wall layer is examined as an extension of the Reynolds stress relaxation analysis of Crow (1967, 1968), who was concerned with the interaction of large-scale disturbances with free space homogeneous, isotropic turbulence. The no-slip condition at the wall results in the formation of acoustic momentum and thermal boundary layers which are subject to the modifying influences of turbulent diffusion normal to the wall. A theoretical model is proposed which incorporates both molecular and turbulence diffusion, and which leads to an analytic representation of the turbulence-controlled acoustic boundary layers. The theory is strictly appropriate at low mean flow Mach numbers, and for acoustic frequencies which are sufficiently large that the widths of these boundary layers do not exceed that of the constant shear stress (or 'logarithmic') region close to the wall. This condition is satisfied in most practical applications and for available experimental data. The discussion is based on arguments originating in the rapid distortion theory of Ribner & Tucker (1952) and Batchelor & Proudman (1954), which have been discussed in detail by Crow (1967, 1968) and by Noir & George (1978) in the absence of boundaries.

The general problem of the interaction of sound with a low Mach number turbulent wall layer is examined in § 2 of this paper. A detailed analytical discussion is given of the effect of turbulence on the momentum boundary layer of the acoustic field, and conditions are obtained under which the proposed theory is expected to be valid. In § 3 the analysis is extended to include the effects of heat transfer by turbulent convection, leading to a modified representation of the thermoacoustic boundary layer. When the turbulence friction velocity v_* is allowed to vanish, the analytical representations of these boundary layers reduce to those describing the classical Kirchhoff–Stokes exponential forms, and the theory provides a transition formula connecting the opposite extremes in which the boundary layers are controlled respectively by molecular and turbulent diffusion. Application is made (§ 4) to the theory of sound propagation in turbulent pipe flow; excellent agreement is obtained between predicted attenuations and experimental determinations cited above for mean flow Mach numbers less than 0·3. This is consistent with the low Mach number approximation.

This favourable agreement gives some confidence in an application of the present theory – whose specialized conclusions will be reported elsewhere — to the calculation of the wavenumber–frequency spectrum of the surface pressure beneath a turbulent boundary layer. The surface pressure spectrum predicted by Ffowcs Williams (1965), and subsequently in more detail by Bergeron (1974), exhibits a singularity at the critical wavenumber $k = \omega/c$ (where ω is the radian frequency and c the speed of sound), corresponding to sound waves which propagate along the boundary layer parallel to the wall. These authors took no account of the interactions of such waves with the boundary-layer turbulence through which they pass, nor of the fluctuations in the surface shear stress 'dipoles' (Curle 1955), which must act to alleviate the secular growth in the pressure signature at the critical wavenumber.

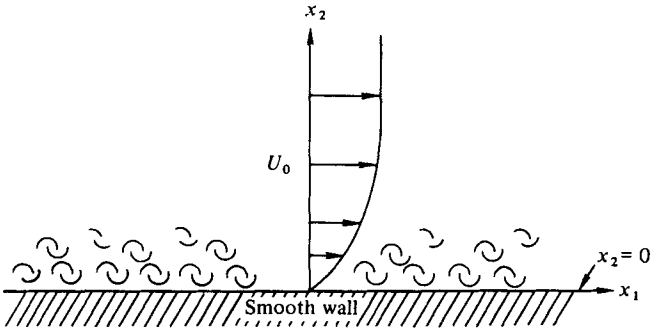

FIGURE 1. Schematic illustration of the configuration of the wall-turbulence shear flow.

2. Momentum transfer in the acoustic boundary layer

Consider the low Mach number wall-turbulence shear flow depicted schematically in figure 1. The mean flow is parallel to the x_1 axis of a rectangular co-ordinate system (x_1, x_2, x_3), and is confined to the region $x_2 > 0$ adjacent to a smooth, rigid wall occupying the plane $x_2 = 0$. The mean velocity is denoted by $U_0(x_2)$, and is assumed to be effectively independent of x_1 for distances comparable with all relevant length scales of the problem. We examine the interaction of the shear flow with an acoustic field whose wavelength greatly exceeds the width L, say, of the constant shear stress region of the wall turbulence. In boundary-layer flow $L \gtrsim \delta_*$, the displacement thickness, and in turbulent pipe flow L is about one tenth of the pipe radius (Hinze 1975, § 7). For $x_2 \gg L$ we write $U_0 \equiv U =$ constant.

When sound is incident on turbulence located in free space the consequent straining of the turbulent vortex lines produces variations in the Reynolds stress which are *coherent* over distances of the order of the acoustic wavelength. The fluctuating Reynolds stress τ_{ij} is defined by

$$\tau_{ij} = \rho v_i v_j - \langle \rho v_i v_j \rangle, \tag{2.1}$$

where ρ is the fluid density, **v** the velocity relative to the local mean flow, and the angle brackets $\langle\ \rangle$ denote an ensemble average in the *absence* of the incident sound. The interaction will result in a significant transfer of energy from the acoustic field to the turbulence provided that the relaxation time, during which nonlinear processes smooth out coherent variations in τ_{ij}, is small compared with the period of the sound wave; otherwise the periodic straining of the vortex lines is reversible, and acoustic energy losses arise only through the generation of scattered, secondary sound waves. When the wavelength is large compared with the characteristic scale L, scattering is of minimal significance (Noir & George 1978) and will be ignored in the present discussion.

In the presence of a rigid wall an acoustic boundary layer is formed at the surface where the no-slip condition must be fulfilled. As a result the length scale of the acoustic perturbation is now very much smaller than the acoustic wavelength, and the corresponding rate of strain of the wall turbulence is likely to be several orders of magnitude larger than it would be in the absence of the wall. A greatly increased rate of energy transfer from the sound to the turbulence may therefore be anticipated. In order to

quantify the interaction mechanism we introduce a formal extension of the free space analyses of Crow (1967, 1968) and Noir & George (1978).

Let $\bar{\tau}_{ij}$ denote the *coherent* component of the Reynolds stress:

$$\bar{\tau}_{ij} = \overline{\rho v_i v_j} - \langle \rho v_i v_j \rangle, \tag{2.2}$$

where the overbar defines an ensemble average in the *presence* of the incident sound. The rate of change of $\bar{\tau}_{ij}$ will be expressed in terms of the difference in the competing effects of the straining of the turbulence by the sound, which induces the *coherent* perturbation in the stress, and the tendency for that coherence to decay through nonlinear interactions of the components of the turbulence and viscous dissipation (cf. Crow 1967, 1968; Noir & George 1978). This difference is formally represented in a manner consistent with linear acoustics by the following linear relation between $\bar{\tau}_{ij}$ and the acoustic perturbation velocity $\bar{\mathbf{u}}$:

$$\frac{D}{Dt}\bar{\tau}_{ij} = -\rho_0 \langle q^2 \rangle A_{ijkl}\left(\frac{\partial \bar{u}_k}{\partial x_l} + \frac{\partial \bar{u}_l}{\partial x_k}\right) - \sigma(x_2)\bar{\tau}_{ij}, \tag{2.3}$$

where

$$\frac{D}{Dt} \equiv \frac{\partial}{\partial t} + U_0(x_2)\frac{\partial}{\partial x_1}. \tag{2.4}$$

In equation (2.3) $\langle q^2 \rangle \equiv \langle q(x_2)^2 \rangle = \langle v_i v_i \rangle$, and ρ_0 is the mean fluid density which is taken to be constant. Within the logarithmic region of the turbulent wall layer, for which $30\nu/v_* \lesssim x_2 \lesssim L$ (ν being the kinematic viscosity and v_* the friction velocity) it is known from experiment that $\langle q^2 \rangle \simeq 6 - 10 v_*^2$ (Hinze 1975, pp. 642, 728).

The tensor coefficient A_{ijkl}, which also depends on x_2, has components of order unity, and determines the coherent change in τ_{ij} which occurs when nonlinear turbulence interactions are ignored. In principle A_{ijkl} may be expressed in terms of assumed properties of the turbulence in the wall layer by the methods of rapid-distortion theory (Ribner & Tucker 1952; Batchelor & Proudman 1954). For example, in the very special case of homogeneous, isotropic turbulence Noir & George (1978) have used the results of Ribner & Tucker to show that at large distances from the wall

$$A_{ijkl} = \tfrac{1}{30}[4\delta_{ik}\delta_{jl} + 7\delta_{ij}\delta_{kl}]. \tag{2.5}$$

The final term on the right-hand side of (2.3) accounts for the decay of $\bar{\tau}_{ij}$ due to its departure from the null equilibrium value, and arises from viscous dissipation and nonlinear processes ignored in rapid distortion theory. The time scale of this decay is of the same order as that which characterises the evolution of the turbulence, i.e.

$$\sigma(x_2) \sim v_*/l, \tag{2.6}$$

where l is an appropriate turbulence length scale: within the constant shear stress region $l \sim x_2$ (Hinze 1975, § 7). In general $\sigma(x_2)$ is also a function of i, j, but it will suffice to suppress an explicit representation of this dependence, since only $\bar{\tau}_{i2}$, with the i direction in the plane of the wall, will turn out to be relevant in the present discussion.

Consider next an acoustic disturbance of radian frequency $\omega > 0$. In the vicinity of the wall set

$$\begin{pmatrix} \bar{u}_i \\ \bar{p} \\ \bar{\tau}_{ij} \end{pmatrix} = \begin{pmatrix} \hat{\bar{u}}_i(x_2) \\ \hat{\bar{p}}(x_2) \\ \hat{\bar{\tau}}_{ij}(x_2) \end{pmatrix} \exp\{i(k_i x_i - \omega t)\}, \tag{2.7}$$

where p is the acoustic pressure, and k_i is the acoustic wavenumber in the i direction parallel to the wall, so that $|k_i| \lesssim \omega/c$, c being the speed of sound. For the remainder of this section the suffix i will represent a fixed direction in the (x_1, x_3) plane to which the summation convention for repeated suffixes will *not* apply. The assumption of long acoustic wavelength introduced above implies that

$$k_i L \ll 1. \tag{2.8}$$

To determine the behaviour of $\hat{\bar{u}}_i \equiv \hat{\bar{u}}_i(x_2)$ near the wall a 'boundary layer' type of approximation which is valid at low Mach numbers will now be developed. Variations in the properties of the mean flow due to compressibility are neglected, in which case near the wall the i component of the momentum equation assumes the form

$$\frac{D}{Dt}\overline{(\rho v_i)} + \frac{\partial \bar{p}}{\partial x_i} = -\frac{\partial \bar{\tau}_{ij}}{\partial x_j} + \rho_0 \nu \nabla^2 \bar{u}_i + \frac{\rho_0 \nu}{3}\frac{\partial}{\partial x_i}(\operatorname{div} \bar{\mathbf{u}}) \tag{2.9}$$

for a Stokesian fluid. Within the turbulent wall layer (2.7) implies that

$$\begin{aligned} -\frac{\partial \bar{\tau}_{ij}}{\partial x_j} &= -\left\{\frac{\partial \hat{\bar{\tau}}_{i2}}{\partial x_2} + ik_i \hat{\bar{\tau}}_{ii}\right\} \exp\{i(k_i x_i - \omega t)\} \quad \text{(no summation)} \\ &\simeq -\frac{\partial \hat{\bar{\tau}}_{i2}}{\partial x_2} \exp\{i(k_i x_i - \omega t)\} \end{aligned} \tag{2.10}$$

since $k_i \delta_A \ll 1$, δ_A being the width of the acoustic boundary layer. Similarly the leading boundary-layer contribution from the viscous terms of (2.9) is provided by

$$\rho_0 \nu \nabla^2 \bar{u}_i \simeq \rho_0 \nu \, \partial^2 \bar{u}_i / \partial x_2^2.$$

Density fluctuations give a second-order contribution in the first term on the left of (2.9), so that on substituting from (2.7) we have within the acoustic boundary layer

$$-i\omega\left(\hat{\bar{u}}_i - \frac{k_i}{\rho_0 \omega}\hat{\bar{p}}\right) = -\frac{1}{\rho_0}\frac{\partial \hat{\bar{\tau}}_{i2}}{\partial x_2} + \nu \frac{\partial^2 \hat{\bar{u}}_i}{\partial x_2^2}, \tag{2.11}$$

where, in addition, we have set $D/Dt = \partial/\partial t$, with an error $\sim O(M_0)$ relative to unity, $M_0 = U_0/c$ being the local mean flow Mach number which is assumed to be small.

In this equation variations in the pressure $\bar{p}$ are insignificant when the acoustic wavelength is large. The final term on the right-hand side involving the kinematic viscosity ν becomes comparable with the Reynolds stress term for $v_* x_2/\nu \lesssim 30$, where viscous diffusion of momentum is no longer small in comparison with turbulent convection. Within the viscous sublayer ($v_* x_2/\nu < 5$–7) convection by the turbulence is negligible.

When similar approximations are applied to the $i2$-component of the Reynolds stress equation (2.3) we obtain in the boundary layer

$$\{\sigma(x_2) - i\omega\}\hat{\bar{\tau}}_{i2} = -\rho_0 \langle q^2 \rangle D_i \frac{\partial \hat{\bar{u}}_i}{\partial x_2}, \tag{2.12}$$

where $D_i \sim O(1)$ and is given by

$$D_i = A_{i22i} + A_{i2i2} \quad \text{(no summation)}. \tag{2.13}$$

Elimination of the shear stress fluctuation $\hat{\tau}_{i2}$ between equations (2.11), (2.12) leads to the following boundary-layer equation describing the variation of $\overline{u}_i$ close to the wall:

$$\frac{\partial}{\partial x_2}\left\{\left(\nu+\frac{\langle q^2\rangle D_i(x_2)}{[\sigma(x_2)-i\omega]}\right)\frac{\partial\hat{\overline{u}}_i}{\partial x_2}\right\}+i\omega\left(\hat{\overline{u}}_i-\frac{k_i}{\rho_0\omega}\hat{\overline{p}}\right)=0. \tag{2.14}$$

In the exterior flow region ($x_2 \gg \delta_A$) the first term on the left, which accounts for the lateral diffusion of momentum, is negligible, and (2.14) yields the free field relation

$$\hat{\overline{u}}_i=\frac{k_i}{\rho_0\omega}\hat{\overline{p}}. \tag{2.15}$$

Actually this result is strictly valid only in the absence of acoustic interactions with the free-stream turbulence. The inclusion of such effects in the analysis results in a modified relation between $\hat{\overline{u}}_i$, $\hat{\overline{p}}$ which differs from (2.15) by terms of relative order $\sim m_*^3 \ll 1$ ($m_* = v_*/c$) (Noir & George 1978).

The diffusive term on the left of (2.14) accounts for the rapid variation of $\hat{\overline{u}}_i$ at the wall, the diffusivity

$$\epsilon(x_2)=\nu+\frac{\langle q(x_2)^2\rangle D_i(x_2)}{\sigma(x_2)-i\omega} \tag{2.16}$$

being the sum of the molecular diffusivity ν and a frequency-dependent turbulent diffusivity ϵ_m, say. Viscous diffusion predominates within the viscous sublayer, where ϵ_m is very small, and equation (2.14) reduces to that describing the Stokes laminar boundary layer (Lighthill 1978, page 130).

The detailed behaviour of $\hat{\overline{u}}_i$ depends on the way in which ϵ_m varies with x_2, and this apparently precludes further analytical discussion of the general case. Progress is possible, however, in the *quasi-static* approximation to the turbulent diffusivity, i.e. when its dependence on ω is neglected. This approximation, whose validity will be examined *a posteriori*, requires that the acoustic period is large compared with the turbulence time scale, i.e. that

$$\omega \ll \sigma(x_2) \tag{2.17}$$

in the range of values of x_2 for which the acoustic–turbulence interaction is significant. Equation (2.12) indicates that in this approximation the shear stress $\hat{\tau}_{i2}$ is in phase with the acoustic rate of strain, its value adjusting instantaneously with the acoustic field.

Quasi-static approximation to the momentum diffusivity

It is convenient to introduce a dimensionless parameter κ by means of the definition

$$\kappa=\frac{\langle q^2\rangle D_i}{\sigma v_* x_2}, \tag{2.18}$$

in which case it follows from (2.14) that in the quasi-static approximation

$$\frac{\partial}{\partial x_2}\left\{(\nu+\kappa v_* x_2)\frac{\partial\hat{\overline{u}}_i}{\partial x_2}\right\}+i\omega\left(\hat{\overline{u}}_i-\frac{k_i\hat{\overline{p}}}{\rho_0\omega}\right)=0, \tag{2.19}$$

where

$$\epsilon_m=\kappa v_* x_2. \tag{2.20}$$

It is now postulated that ϵ_m does not differ substantially in magnitude from the eddy viscosity which characterizes the behaviour of the mean velocity profile close

to the wall; indeed, as $\omega \to 0$ we recover from (2.19) the equation for the mean velocity profile in the presence of a mean pressure gradient $ik_i\hat{\bar{p}} \sim \partial\bar{p}/\partial x_i$. Within the logarithmic region, where diffusion is controlled by turbulent convection ($30\nu/v_* \lesssim x_2 \lesssim L$), κ coincides with the von Kármán universal constant ($\kappa \simeq 0{\cdot}4$), and ϵ_m varies linearly with x_2 (Hinze 1975, pp. 645, 730). For smaller values of x_2, $\epsilon_m \propto x_2^n$ ($n \geqslant 2$). We shall ignore such departures from linearity, and assume that κ may be taken as constant within the acoustic boundary layer. The error involved in this further approximation will be shown to be insignificant.

Recalling that $\hat{\bar{p}}$ does not vary across the boundary layer, we find that when κ is constant equation (2.19) can be solved in closed form in terms of the Hankel function $H_0^{(1)}(z)$. The solution which satisfies the no-slip condition at the wall and tends to the free field perturbation velocity $k_i\hat{\bar{p}}/\rho_0\omega$ is given by

$$\hat{\bar{u}}_i = \frac{k_i\hat{\bar{p}}}{\rho_0\omega}\left\{1 - \frac{H_0^{(1)}\left[\left(\left(\frac{\kappa v_* x_2}{\nu}+1\right).\frac{4i\omega\nu}{\kappa^2 v_*^2}\right)^{\frac{1}{2}}\right]}{H_0^{(1)}\left[\left(\frac{4i\omega\nu}{\kappa^2 v_*^2}\right)^{\frac{1}{2}}\right]}\right\}, \tag{2.21}$$

where $\mathrm{Im}\{(4i\omega\nu/\kappa^2 v_*^2)^{\frac{1}{2}}\} > 0$. Observe that this result reduces to the exponential Stokes layer form as the turbulence intensity tends to zero ($v_* \to 0$).

The width δ_A of the acoustic boundary layer defined by (2.21) depends on the value of the dimensionless parameter $4\omega\nu/\kappa^2 v_*^2$, which can also be expressed in the form

$$\frac{4\omega\nu}{\kappa^2 v_*^2} = \frac{4}{\kappa^2\beta^2}.\frac{St}{Re}, \tag{2.22}$$

in terms of Reynolds and Strouhal numbers defined respectively by

$$Re = \frac{U\Delta}{\nu}; \quad St = \frac{\omega\Delta}{U}, \tag{2.23}$$

where Δ is an arbitrary length scale, and $\beta \sim 0{\cdot}04$ is approximately constant, with $v_* = \beta U$ (Hinze 1975, § 7).

The real and imaginary parts of the boundary-layer profiles are illustrated in figure 2 for $4\omega\nu/\kappa^2 v_*^2 = 0{\cdot}1$, 1, 10, as functions of $\kappa v_* x_2/\nu$ and $v_* x_2/\nu$, the latter scale being calculated on the assumption that $\kappa = 0{\cdot}4$ (the function $H_0^{(1)}(xi^{\frac{1}{2}})$ is given in tabular form by Jahnke & Emde 1945). The dashed curves in this figure represent the component of velocity which is in phase with the pressure gradient $ik_i\hat{\bar{p}}$, and determine the rate at which the acoustic energy is dissipated through the action of viscosity and conversion to turbulence. The width of the boundary layer may be defined by the value of x_2 at which the real part of the velocity first attains its free field value (unity in the figure). A detailed inspection of the numerical results reveals that in the range $0{\cdot}1 \leqslant 4\omega\nu/\kappa^2 v_*^2 \leqslant 30$, expected to be important in applications (see § 4), δ_A is well approximated by the formula

$$\frac{\kappa v_* \delta_A}{\nu} = 10{\cdot}8\left(\frac{4\omega\nu}{\kappa^2 v_*^2}\right)^{-0{\cdot}71}. \tag{2.24}$$

The importance of the turbulent fluctuations in determining the structure of the boundary layer may be surmised from a consideration of the dissipation rate. At low

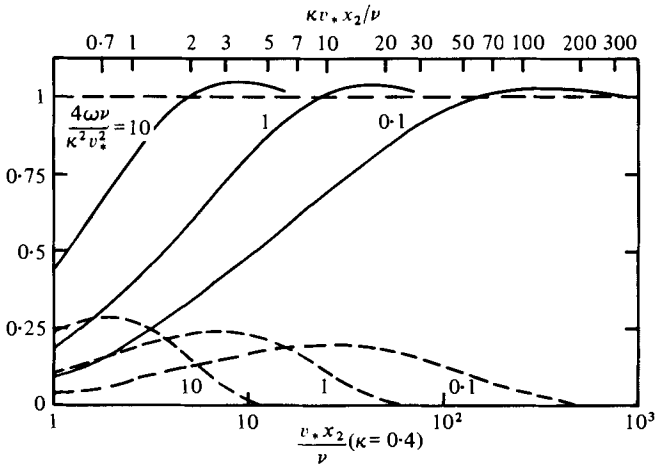

FIGURE 2. Acoustic momentum boundary-layer profiles $\hat{u}_i/(k_i\hat{\overline{p}}/\rho_0\omega)$ determined by equation (2.21): ——, Re $\{\hat{u}_i/(k_i\hat{\overline{p}}/\rho_0\omega)\}$; – – – –, Im $\{-\hat{u}_i/(k_i\hat{\overline{p}}/\rho_0\omega)\}$.

frequencies dissipation occurs principally through the ceding of energy to the turbulent field; with increasing frequency, however, a progressively larger fraction of the dissipated energy is converted directly into heat in the viscous sublayer. The rate of dissipation per unit area of the wall, E, say, is given by

$$E = \int_0^\infty \overline{u}_i \frac{\partial \overline{p}}{\partial x_i}\, dx_2, \tag{2.25}$$

where the real parts of $\overline{u}_i$, $\overline{p}$, defined in (2.7), are to be taken. The integral can be evaluated from the solution (2.21) to yield

$$E = \frac{1}{2\rho_0\omega}\cdot\left(\frac{\nu}{2\omega}\right)^{\frac{1}{2}}\left|\frac{\partial\overline{p}}{\partial x_1}\right|^2 \mathrm{Re}\left\{\sqrt{(2i)}\,\frac{H_1^{(1)}\left[\left(\frac{4i\omega\nu}{\kappa^2 v_*^2}\right)^{\frac{1}{2}}\right]}{H_0^{(1)}\left[\left(\frac{4i\omega\nu}{\kappa^2 v_*^2}\right)^{\frac{1}{2}}\right]}\right\}. \tag{2.26}$$

As $v_* \to 0$ (absence of turbulent fluctuations) the real part of the term in the curly brackets of this equality is ultimately equal to unity, and (2.26) reduces to

$$E_\nu = \frac{1}{2\rho_0\omega}\left(\frac{\nu}{2\omega}\right)^{\frac{1}{2}}\left|\frac{\partial\overline{p}}{\partial x_1}\right|^2, \tag{2.27}$$

which is the viscous rate of dissipation per unit area (Lighthill 1978, p. 133). The ratio E/E_ν is accordingly a measure of the influence of the boundary-layer turbulence on the sound, and its variation as a function of $4\omega\nu/\kappa^2 v_*^2$ is depicted in figure 3. The greatest departures from the viscous controlled boundary layer occur for $4\omega\nu/\kappa^2 v_*^2 < 1$, and E/E_ν is within 50 % of its high frequency asymptote for $4\omega\nu/\kappa^2 v_*^2 > 1{\cdot}8$.

Now an examination of the experimental results of Schubauer (1954) and Laufer (1954), reproduced on pp. 644 and 731 of Hinze (1975), indicates that $\kappa \simeq$ const. $\simeq 0{\cdot}4$ for $v_* x_2/\nu \gtrsim 30$, and diminishes rapidly to zero for smaller values of x_2. Hence, using (2.24), the condition $4\omega\nu/\kappa^2 v_*^2 < 1$ for the boundary layer to be effectively controlled by turbulent diffusion becomes

$$\frac{v_*\delta_A}{\nu} \gtrsim 27, \tag{2.28}$$

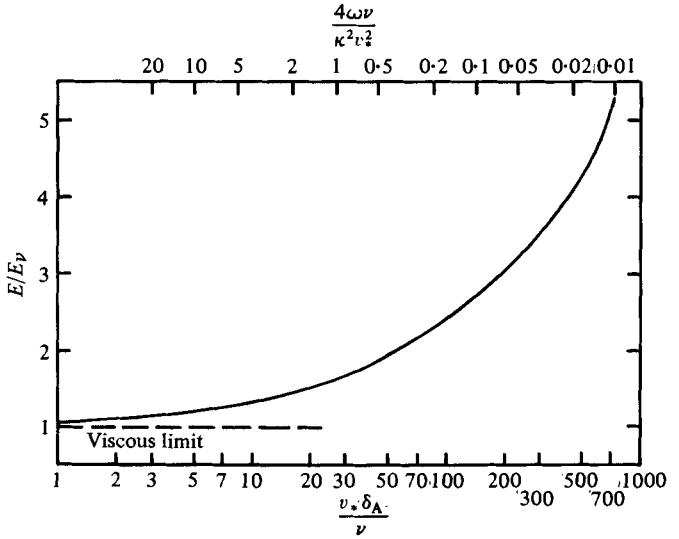

FIGURE 3. Rate of dissipation of acoustic energy per unit area of the wall due to viscosity and conversion to turbulence (E) normalized with respect to the viscous dissipation E_ν in the absence of turbulence.

i.e. that the boundary layer should reach out at least to the inner edge of the logarithmic region of the wall shear flow. For such values of δ_A it may be assumed that $\kappa = 0{\cdot}4$, and indeed this value can also be used in the high frequency region since we have already seen from figure 3 that the departures from the Stokes layer asymptotic limit are small for $4\omega\nu/\kappa^2 v_*^2 > 1$. The variation of E/E_ν as a function of $v_*\delta_A/\nu$ ($\kappa = 0{\cdot}4$) is also given in figure 3.

It remains to establish the validity of the quasi-static approximation (2.17) used in the derivation of the boundary-layer equation (2.19). Use of (2.18) shows that the necessary condition is that

$$\omega \ll \frac{\langle q^2 \rangle D_i}{\kappa v_* x_2}, \tag{2.29}$$

for values of $x_2 < \delta_A$. From (2.24) it is seen that this will be satisfied provided that

$$\frac{4\omega\nu}{\kappa^2 v_*^2} \ll \left(\frac{0{\cdot}37\langle q^2 \rangle D_i}{\kappa^2 v_*^2}\right)^{3{\cdot}45}. \tag{2.30}$$

Within the logarithmic region of the wall layer $\langle q^2 \rangle$ is typically of order $6v_*^2$. The value of the coefficient D_i defined in (2.13) is more difficult to estimate, but it probably does not differ greatly from the value given by equation (2.5) for homogeneous, isotropic turbulence, viz. $D_i = \frac{4}{30}$. Taking these values, and setting $\kappa = 0{\cdot}4$, we find from (2.30)

$$\frac{4\omega\nu}{\kappa^2 v_*^2} \ll 8{\cdot}35. \tag{2.31}$$

It has already been argued that the acoustic–turbulence interaction is important only for $4\omega\nu/\kappa^2 v_*^2 < 1$. Thus it may be tentatively concluded that the quasi-static approximation (2.20) for the turbulence diffusivity ϵ_m is justified for constant κ at all

frequencies for which $\delta_A < L$, i.e. for which the acoustic boundary layer does not extend beyond the logarithmic region of the mean flow. Using (2.24) this condition can be expressed in the form

$$\frac{4\omega\nu}{\kappa^2 v_*^2} > \frac{104}{\left(\frac{v_* L}{\nu}\right)^{1\cdot41}}, \tag{2.32}$$

in general $v_* L/\nu > 300$, and (2.32) is likely to be satisfied over a wide range of practical situations, including the experimental data examined later in this paper.

3. Heat transfer within the acoustic boundary layer

The analysis of § 2 has taken no account of the periodic variations in fluid temperature arising from the compressions and rarefactions of the wall shear flow by the sound. The classical Kirchhoff–Stokes theory predicts that the dissipation involved in the establishment of a fluctuating thermal boundary layer is comparable in magnitude to that due to viscosity. To examine the situation in the presence of wall turbulence we shall assume that the transfer of heat is described by the quasi-static diffusion equation

$$\rho T \frac{Ds}{Dt} = \frac{\partial}{\partial x_j}\left(K \frac{\partial T}{\partial x_j}\right), \tag{3.1}$$

in which T is the temperature and s is the specific entropy. The transport coefficient K is defined by

$$K = \rho c_p(\chi + \epsilon_\theta), \tag{3.2}$$

where χ is the thermometric conductivity, c_p the specific heat at constant pressure, and ϵ_θ is a thermal eddy diffusivity. At points within the logarithmic region of the wall flow K is expected to vary linearly with x_2 (see, e.g., Rotta 1960), and we shall write

$$\epsilon_\theta = \frac{\epsilon_m}{P_t} \equiv \frac{\kappa v_* x_2}{P_t}, \tag{3.3}$$

P_t being the turbulence Prandtl number. Blom (1970) has concluded from a survey of available experimental data for air that $P_t \sim 0{\cdot}7$–$0{\cdot}8$. Bradshaw (1977) quotes a value of $0{\cdot}91$, however. In the application to be described below such small differences in the value of P_t have a relatively minor effect on the theoretical predictions, and we shall accordingly assume that $P_t = 0{\cdot}8$.

Use of the thermodynamic relation

$$T\,ds = c_p dT - \frac{1}{\rho} dp, \tag{3.4}$$

enables (3.1) to be reduced to the boundary-layer form

$$\frac{\partial}{\partial x_2}\left\{\left(\chi + \frac{\kappa v_* x_2}{P_t}\right)\frac{\partial \hat{\hat{T}}}{\partial x_2}\right\} + i\omega\left(\hat{\hat{T}} - \frac{\hat{\hat{p}}}{\rho_0 c_p}\right) = 0, \tag{3.5}$$

where $\hat{\hat{T}}$ is the acoustic temperature fluctuation defined as in (2.7), the $O(M_0)$ convective component of the material derivative D/Dt has been discarded, and variations in the mean density can be ignored. As in § 2, $\hat{\hat{p}}$ may be regarded as constant across the

boundary layer, and the solution of (3.5) which satisfies the usual wall condition of vanishing fluctuating temperature assumes a form analogous to (2.21):

$$\hat{\bar{T}} = \frac{\hat{\bar{p}}}{\rho_0 c_p}\left\{1 - \frac{H_0^{(1)}\left[\left(\left(\frac{\kappa v_* x_2}{\chi P_t}+1\right).\frac{4i\omega\chi P_t^2}{\kappa^2 v_*^2}\right)^{\frac{1}{2}}\right]}{H_0^{(1)}\left[\left(\frac{4i\omega\chi P_t^2}{\kappa^2 v_*^2}\right)^{\frac{1}{2}}\right]}\right\}. \tag{3.6}$$

When $P_t = 0{\cdot}8$, χP_t^2 does not differ significantly from ν for air, and the principal characteristics of this solution are therefore very similar to those already discussed for the velocity distribution (2.21).

4. Attenuation of sound in turbulent pipe flow

The results of §§ 2, 3 will now be applied to the propagation of sound in a smooth-walled pipe of uniform cross-sectional area $\mathscr{A}$ in the presence of a low Mach number fully developed turbulent mean flow. This will permit comparison of predictions of the theoretical model with existing experimental results. Attention is confined to one-dimensional propagation parallel to the axis of the pipe which is taken in the x_1 direction.

Integration of the x_1 component of the momentum equation (2.9) across the pipe gives

$$\frac{D\mathscr{M}}{Dt} + \frac{\partial P}{\partial x_1} = -\frac{1}{\mathscr{A}}\frac{\partial}{\partial x_1}\int \bar{\tau}_{11}\,dS - \rho_0 \frac{\nu a}{\mathscr{A}}\left(\frac{\partial \bar{u}_1}{\partial x_2}\right)_{x_2=0}, \tag{4.1}$$

where mean viscous stresses in the flow are neglected in comparison with the normal turbulent stress $\bar{\tau}_{11}$. In equation (4.1)

$$\begin{pmatrix} P \\ \mathscr{M} \end{pmatrix} = \frac{1}{\mathscr{A}}\int \begin{pmatrix} \bar{p} \\ \bar{\rho}\bar{v} \end{pmatrix} dS, \tag{4.2}$$

dS is the cross-section area element, a the perimeter of the pipe, and, except in regions very close to the wall, the mean velocity U may be regarded as constant. The derivative $(\partial \bar{u}_1/\partial x_2)_{x_2=0}$ is evaluated at the pipe wall, x_2 being a temporary local co-ordinate normal to the wall ($x_2 = 0$).

In the same approximation the integrated form of the continuity equation can be set in the form

$$\frac{1}{\bar{c}^2}\frac{DP}{Dt} + \frac{\partial \mathscr{M}}{\partial x_1} = \frac{1}{\mathscr{A} c_p}\int \rho \frac{D\bar{s}}{Dt}\,dS, \tag{4.3}$$

variations in the mean thermodynamic properties of the flow being small at low Mach numbers. The integral in (4.3) is simplified by means of equations (3.1), (3.2):

$$\frac{1}{\mathscr{A} c_p}\int \rho \frac{D\bar{s}}{Dt}\,dS = -\frac{a\rho_0\chi}{\mathscr{A} T_0}\left(\frac{\partial \bar{T}}{\partial x_2}\right)_{x_2=0} + \frac{\rho_0}{\mathscr{A}}\frac{\partial^2}{\partial x_1^2}\int \frac{\epsilon_\theta \bar{T}}{T_0}.dS, \tag{4.4}$$

where T_0 is the mean temperature. In evaluating the integral on the right-hand side we write $\epsilon_\theta = \bar{\epsilon}_\theta = \text{const.}$, since the diffusivity is effectively uniform within the core of the pipe flow. An equally adequate approximation permits the replacement of $\bar{T}/T_0$

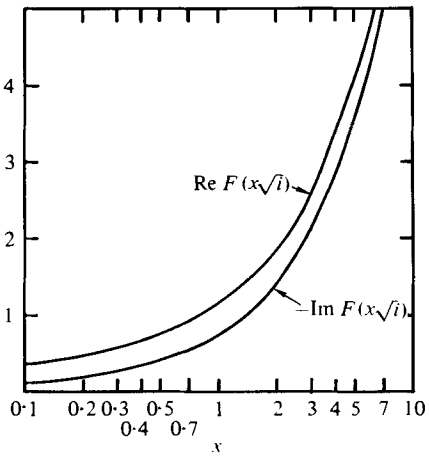

FIGURE 4. Real and imaginary parts of $F(x\sqrt{i})$ defined in equation (4.9).

in the integrand by the adiabatic representation $(\gamma-1)P/\rho_0 c^2$, γ being the ratio of the specific heats, so that (4.3) now reduces to

$$\frac{1}{c^2}\frac{DP}{Dt}+\frac{\partial \mathscr{M}}{\partial x_1}=-\frac{a\rho_0\chi}{\mathscr{A}T_0}\left(\frac{\partial \overline{T}}{\partial x_2}\right)_{x_2=0}+\frac{(\gamma-1)\bar{\epsilon}_\theta}{c^2}\frac{\partial^2 P}{\partial x_1^2}, \tag{4.5}$$

and the elimination of $\mathscr{M}$ between this result and equation (4.1) gives finally

$$\left(\frac{1}{c^2}\frac{D^2}{Dt^2}-\frac{\partial^2}{\partial x_1^2}\right)P=\frac{1}{\mathscr{A}}\frac{\partial^2}{\partial x_1^2}\int \bar{\tau}_{11}\,dS+\frac{(\gamma-1)\bar{\epsilon}_\theta}{c^2}\frac{D}{Dt}\cdot\frac{\partial^2 P}{\partial x_1^2}$$
$$+\frac{a\rho_0}{\mathscr{A}}\left\{\frac{\nu\partial}{\partial x_1}\left(\frac{\partial \overline{u}_1}{\partial x_2}\right)-\frac{\chi}{T_0}\frac{D}{Dt}\left(\frac{\partial \overline{T}}{\partial x_2}\right)\right\}_{x_2=0}. \tag{4.6}$$

In order to obtain the dispersion relation between the frequency ω and the wavenumber k in the case of an acoustic field which varies in proportion to $\exp\{i(kx_1-\omega t)\}$, as in (2.7), the boundary-layer solutions (2.21), (3.6) must first be used to express the surface derivatives in (4.6) in terms of $P\equiv\overline{p}$. The contribution from the integrated normal stress $\bar{\tau}_{11}$ can be estimated from equation (2.3) by setting $\overline{u}_1=k\overline{p}/\rho_0\omega$ within the core region. In this way we obtain

$$k^2-\left(\frac{\omega}{c}-Mk\right)^2=\mathscr{L}(\omega), \tag{4.7}$$

where $M=U/c$, and $\mathscr{L}(\omega)$ is determined by the terms on the right of (4.6) and is responsible for the attenuation of the sound by the acoustic–turbulence interaction. In simplifying the general expression for $\mathscr{L}$ we must set $M=0$, $|k|=\omega/c$ in order to achieve consistency with the boundary-layer approximations of §§ 2, 3, in which case

$$\mathscr{L}(\omega)=\frac{i\omega^3}{c^4}\left\{\frac{2A_{1111}\overline{q^2}}{\overline{\sigma}-i\omega}+\bar{\epsilon}_\theta(\gamma-1)\right\}$$
$$+\frac{i\omega\kappa m_* a}{2c\mathscr{A}}\left\{F\left[\left(\frac{4i\omega\nu}{\kappa^2 v_*^2}\right)^{\frac{1}{2}}\right]+\frac{(\gamma-1)}{P_t}F\left[\left(\frac{4i\omega\chi P_t^2}{\kappa^2 v_*^2}\right)^{\frac{1}{2}}\right]\right\}, \tag{4.8}$$

where $m_*=v_*/c$, and an overbar now denotes a core-averaged quantity.

The complex-valued function $F(x\sqrt{i})$ is defined by

$$F(x\sqrt{i}) = \frac{x\sqrt{i}H_1^{(1)}(x\sqrt{i})}{H_0^{(1)}(x\sqrt{i})}, \tag{4.9}$$

and its real and imaginary parts are plotted in figure 4 for the range of values of x important in applications.

The imaginary part of $\mathscr{L}(\omega)$ determines the magnitude of the acoustic attenuation. Introducing

$$\alpha(\omega) = \mathrm{Im}\left\{\frac{\mathscr{L}(\omega)}{2(\omega/c)}\right\}, \tag{4.10}$$

it follows that in the leading approximation, for small $\alpha(\omega)$, the roots $k = k_\pm$ of the dispersion relation (4.7) are given by

$$(1 \pm M)\, k_\pm = \pm \frac{\omega}{c} \pm i\alpha(\omega), \tag{4.11}$$

the $+/-$ sign being taken according as propagation is in the $+/-$ direction of the x_1 axis, and the wave amplitude decays as

$$\exp\{\pm \alpha(\omega)\, x_1/(1 \pm M)\}.$$

The first term on the right of equation (4.8) arises from the interaction of the sound with the turbulence in the core region of the pipe flow. The corresponding component of the attenuation coefficient $\alpha(\omega)$, viz.

$$\alpha_0 = \frac{A_{1111}\overline{q^2}\overline{\sigma}}{[\overline{\sigma}^2 + \omega^2]} \cdot \frac{\omega^2}{c^3} + \frac{(\gamma - 1)\,\bar{e}_\theta \omega^2}{2c^3}, \tag{4.12}$$

must therefore be identical in form with that describing propagation in free space turbulence.

Noir & George (1978) have discussed the influence of Reynolds stress relaxation on the propagation of sound through homogeneous, isotropic turbulence (with $M \equiv U/c = 0$). In their analysis the frequency ω was assumed to be large compared with the inverse relaxation time $\overline{\sigma}$, and effects of heat transfer were ignored. This gave a frequency-independent expression for the attenuation coefficient which, in the present notation, had the form

$$\alpha_0 = A_{1111}\frac{\overline{\sigma}\overline{q^2}}{c^3}, \tag{4.13}$$

corresponding to the high frequency limit of the first term on the right-hand side of (4.12). It is apparent from equation (4.12) that, except at very low frequencies, attenuation due to Reynolds stress relaxation is a slowly varying function of ω. In particular, the attenuation of *aerodynamically generated sound* (Lighthill 1952), for which $\omega \sim \overline{\sigma}$, is effectively uniform in frequency.

The relative importance of Reynolds stress relaxation and the heat transfer com-

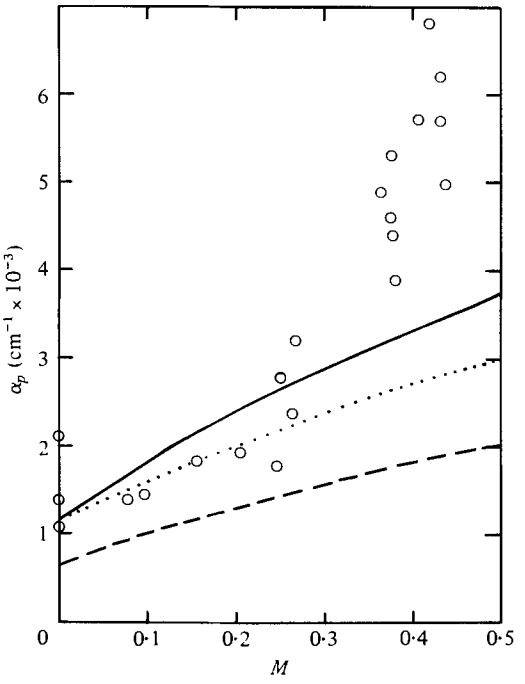

FIGURE 5. Comparison of calculated attenuation coefficient $\alpha_p(\omega)$ with experimental results of Ingard & Singhal (1974) for a fixed frequency $\omega/2\pi = 1100$ Hz and a range of values of the mean flow Mach number M. ——, theory, $P_t = 0{\cdot}8$; . . . ., theory, $P_t = 2{\cdot}5$; – – – –, theory, no heat transfer effects.

ponent of (4.12) can be estimated in terms of the turbulence Mach number $m = \overline{(q^2)}^{\frac{1}{2}}/c$, and correlation length l, say. Observing that $\bar{\epsilon}_\theta \sim \overline{(q^2)}^{\frac{1}{2}}.l$, we have in order of magnitude

$$\frac{\text{heat transfer}}{\text{Reynolds stress relaxation}} \sim \frac{1}{m^2}\left(\frac{\omega l}{c}\right)^2,$$

a ratio which is of order unity for aerodynamic sound. This fact may be significant in resolving some of the differences between theory and experiment reported by Noir & George (1978).

Return now to the pipe flow problem. A simple order of magnitude comparison of the terms on the right of (4.8) confirms that at low Mach numbers the attenuation is controlled by the second, surface interaction component. The attenuation coefficient $\alpha_p(\omega)$, say, therefore becomes

$$\alpha_p(\omega) = \frac{\kappa m_* a}{4\mathscr{A}}.\mathrm{Re}\left\{F\left[\left(\frac{4i\omega\nu}{\kappa^2 v_*^2}\right)^{\frac{1}{2}}\right] + \frac{(\gamma-1)}{P_t}.F\left[\left(\frac{4i\omega\chi P_t^2}{\kappa^2 v_*^2}\right)^{\frac{1}{2}}\right]\right\}. \tag{4.14}$$

It should be noted that the limiting value of this result as $v_* \to 0$ coincides with the Kirchhoff–Stokes attenuation coefficient for sound propagation in the absence of turbulence, since $\mathrm{Re}\,F(x\sqrt{i}) \to x/\sqrt{2}$ as $x \to \infty$.

According to the semi-empirical theory of Ingard & Singhal (1974) the attenuation does not depend on the frequency, and these authors performed experiments in air at a fixed frequency to investigate the dependence of α_p on the mean flow Mach number M.

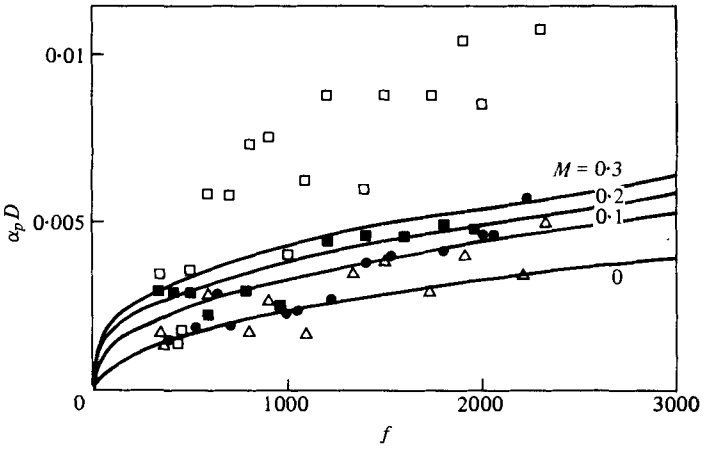

FIGURE 6. Comparison of the calculated normalized attenuation coefficient $\alpha_p D$ and experimental results of Ahrens & Ronneberger (1971) over a range of frequencies f Hz and different mean flow Mach numbers M. Theory, ——; experiment: ●, $M = 0$; △, $M = 0{\cdot}1$; ■, $M = 0{\cdot}2$; □, $M = 0{\cdot}3$.

The experiments involved a standing acoustic wave pattern of frequency $f = 1100$ Hz in a tube of rectangular cross-section $1{\cdot}905 \times 2{\cdot}223\,\mathrm{cm}^2$, the mean velocity varying in the range $U = 0$–$170\,\mathrm{m\,s^{-1}}$. The results are reproduced in figure 5, and it is clear from the spread of the data points that the accuracy of the measurements is not particularly great. The curves plotted in figure 5 are based on equation (4.14). The full curve gives the predicted attenuation for the following parametric values for air:

$$\nu = 0{\cdot}15\,\mathrm{cm^2\,s^{-1}}; \quad \chi = 0{\cdot}21\,\mathrm{cm^2\,s^{-1}}; \quad c = 34\,000\,\mathrm{cm\,s^{-1}};$$

$$\kappa = 0{\cdot}4; \quad P_t = 0{\cdot}8; \quad v_* = 0{\cdot}04U \quad (M = U/c).$$

The dashed curve illustrates the attenuation that would result from shear stress relaxation alone [i.e. from the first term in the brace brackets of (4.14)].

It is apparent that in the low Mach number region $M \leqslant 0{\cdot}3$, say, where theory and experiment may be expected to conform, the dashed (shear stress) curve systematically underpredicts the attenuation. The inclusion of heat transfer effects greatly improves the comparison with experiment. A better fit is obtained in the low Mach number range, however, by taking a larger value for the turbulence Prandtl number, viz., $P_t = 2{\cdot}5$; this corresponds to the dotted curve in figure 5. In any event the agreement between experiment and the theoretical formula (4.14) may be claimed to be satisfactory for $M < 0{\cdot}3$.

A further experimental comparison can be made with the standing wave measurements in air of Ahrens & Ronneberger (1971) who used a smooth-walled circular tube of diameter $D = 7{\cdot}5$ cm. Their experimental results expressed in terms of $\alpha_p D$ are shown in figure 6 for $M = 0$, 0·1, 0·2, 0·3 and a range of values of the frequency $f = \omega/2\pi$. The curves plotted in figure 6 are calculated from (4.14) (with $P_t = 0{\cdot}8$), the case of $M = 0$ being the Kirchoff–Stokes limit obtaining as $v_* \to 0$. Although there is a large spread in the experimental results, a reasonable agreement between theory and experiment is found for $M \leqslant 0{\cdot}2$. Significant differences are apparent for $M = 0{\cdot}3$,

and, as in the case of the Ingard–Singhal experiments, this apparently sets the upper Mach number limit of validity of the present theory.

In conclusion it may be remarked that in their reductions of the experimental data Ingard & Singhal (1974) and Ahrens & Ronneberger (1971) assumed that the amplitudes of the standing wave patterns were proportional to

$$\exp\{\pm\alpha_p x_1/(1\pm M)\},$$

and that α_p is *independent of the direction of propagation*. The validity of this hypothesis may be questioned at the higher Mach numbers, and indicates that a reappraisal of the experimental data may well be necessary for $M \geqslant 0{\cdot}3$. A non-trivial extension of the present theory is also necessary in order to account for the relatively large attenuations observed for such values of M. An approach based on a two-tier model of the boundary-layer equations, involving the matching of solutions in an inner region where convection by the mean flow is small with those valid in an outer region where the convection velocity may be regarded as constant, may possibly be adequate for this purpose.

REFERENCES

Ahrens, C. & Ronneberger, D. 1971 *Acustica* **25**, 150–157.

Batchelor, G. K. 1957 In *Naval Hydrodynamics* (ch. 16). Washington D.C. Nat. Acad. Sci. Publ. 515 Nat. Res. Counc.

Batchelor, G. K. & Proudman, I. 1954 *Quart. J. Mech. Appl. Math.* **7**, 83–103.

Bergeron, R. F. 1974 *J. Acoust. Soc. Am.* **54**, 123–133.

Blom, J. 1970 An experimental determination of the turbulent Prandtl number in a temperature boundary layer. Doctoral thesis, Eindhoven University of Technology.

Bradshaw, P. 1967 *J. Fluid Mech.* **30**, 241–258.

Bradshaw, P. 1977 *Ann. Rev. Fluid Mech.* **9**, 33–54.

Crow, S. C. 1967 *Phys. Fluids* **10**, 1587–1590.

Crow, S. C. 1968 *J. Fluid Mech.* **33**, 1–20.

Curle, N. 1955 *Proc. Roy. Soc.* A **231**, 505–514.

Ffowcs Williams, J. E. 1965 *J. Fluid Mech.* **22**, 507–519.

Hinze, J. O. 1975 *Turbulence*, 2nd ed. McGraw-Hill.

Howe, M. S. 1973 *J. Sound Vib.* **27**, 455–476.

Ingard, U. & Singhal, V. K. 1974 *J. Acoust. Soc. Am.* **55**, 535–538.

Jahnke, E. & Emde, F. 1945 *Tables of Functions*. New York: Dover.

Kraichnan, R. H. 1953 *J. Acoust. Soc. Am.* **25**, 1096–1104.

Laufer, J. 1954 *N.A.C.A. Tech. Note* 2123.

Lighthill, M. J. 1952 *Proc. Roy. Soc.* A **211**, 564–587.

Lighthill, M. J. 1953 *Proc. Camb. Phil. Soc.* **49**, 531–551.

Lighthill, M. J. 1978 *Waves in Fluids*. Cambridge University Press.

Noir, D. T. & George, A. R. 1978 *J. Fluid Mech.* **86**, 593–608.

Ribner, H. S. & Tucker, M. 1952 *N.A.C.A. Tech. Rep.* 2606.

Rotta, J. C. 1960 *Turbulent boundary layers with heat transfer in compressible flow*. AGARD Rep. 281.

Schubauer, G. B. 1954 *J. Appl. Phys.* **25**, 188–196.